RESEARCH ARTICLE

RUNNING HEAD: Effect of adaptive walking assistance in healthy people

Adaptive walking assistance does not impact long-range stride-to-stride autocorrelations in healthy people

Virginie Otlet,[1, 2, 3] Renaud Ronsse,[1, 2, 3]

[1]Institute of Mechanics, Materials, and Civil Engineering, UCLouvain, Louvain-la-Neuve, Belgium
[2] Institute of Neuroscience, UCLouvain, Brussels, Belgium
[3] Louvain Bionics, UCLouvain, Louvain-la-Neuve, Belgium

Correspondence: Virginie Otlet (virginie.otlet@uclouvain.be).

ABSTRACT

Many studies have demonstrated in the past that the level of long-range autocorrelations in series of stride durations, characterizing natural gait variability, is impacted by external constraints, such as treadmill or metronome, or by pathologies, such as Parkinson's or Huntington's disease. Nevertheless, no one has analyzed the effects on this metric of a gait constrained by a robot-mediated walking assistance, which intrinsically tends to normalize the gait pattern. This paper focuses on the influence of a wearable active pelvis orthosis on the level of long-range auto-correlations in series of stride durations. Ten healthy participants, aged between 55 and 77 years, performed four overground walking sessions, wearing this orthosis, and with different assistive parameters. This study showed that the adaptive assistance provided by this device has the potential of improving gait metrics that are typically affected by aging, such as the hip range of motion, walking speed, stride length and duration, without impacting natural gait variability, i.e., the level of long-range autocorrelations in series of stride durations. This combination is virtuous towards the design of an assistive device for people with locomotion disorders resulting in deteriorated levels of long-range autocorrelations, such as patients with Parkinson's disease.

NEW & NOTEWORTHY

This study is the first that investigates the effects of a wearable active pelvis orthosis using an oscillator-based adaptive assistance on the level of long-range autocorrelations in series of stride durations during overground walking. It is also the first to compare the effects of different assistance settings on spatiotemporal gait metrics.

Keywords: long-range autocorrelations; walking assistance; wearable device.

Postprint

INTRODUCTION

Robot-assisted gait training has been developed for more than two decades in order to provide therapies to people with gait disorders. This framework has become attractive because it enables patients to perform a large amount of gait cycle repetitions while reducing physical burden for the therapists (1). It is thus now proposed as a valuable complement to conventional therapies (2). Previous studies reported improvements in specific gait-related metrics of patients, as for example increased gait speed, stride length and balance in people with Parkinson's disease (3), and increased balance and participation in activities of daily living in a post-stroke population (4).

Among the devices used for robot-assisted gait training, the most recent ones are wearable exoskeletons. Some of these devices are developed in order to restore bipedal walking to people with complete or partial spinal cord lesions, as for example the Atalante® (Wandercraft, Paris, France), which has proven to be safe and clinically beneficial for people with complete motor spinal cord injury (5). These devices can also bring solutions to people with mild gait deficiencies, having limited daily activities due to lack of locomotion independence or fear of falling (6). Using a wearable exoskeleton as an assistive device in everyday life has the potential to greatly improve the quality of life for these individuals. With an appropriate control framework, these devices further promote active participation of the user (7), unlike non-wearable devices that can only be used in rehabilitation facilities. Due to their intrinsic wearable nature, they also offer the possibility to be used for gait training in (semi-)ecological environments or at home.

On top of full lower-limb exoskeletons, there exists a wide range of smaller and lighter wearable assistive devices for mild gait disorders, developed for the hip, knee and ankle joints, or a combination thereof (7, 8). Hip assistive devices are likely those with the highest level of maturity in the state of the art. This is due to the proximal location of hip joints – offering to place bulky components in a backpack – and to the ubiquitous role of the hip in sustaining locomotion rhythmicity (9). There is nowadays a convergence of results – obtained by different teams using different devices – showing that providing flexion/extension assistance to the hip induces an increase in gait speed, gait symmetry and/or a decrease in metabolic cost of walking in people with various gait disorders (10–13). Similar results have been reported with devices assisting the ankle joint in dorsi- and plantarflexion with healthy (14) and post-stroke people (15). Finally, an exoskeleton assisting both hips and knees showed a trend towards an increased walking speed and endurance in people with various walking pathologies (16).

In all studies mentioned above, the effect of the device was studied on gait metrics capturing an instantaneous behavior, possibly after a familiarization or learning phase. In the present paper, we aim at extending these investigations on a subtler property of gait motor control, i.e., the presence of long-range autocorrelations (LRA) in series of consecutive stride durations. LRA are present in many periodic physiological signals – such as heartbeat, neural activities, breathing, and gait (17). In the particular case of walking, the presence of LRA in series of stride durations captures that the duration of a given stride shows statistical correlation with a long series of previous ones, including those that occurred several minutes ago (17). Several studies have demonstrated that LRA-related metrics can capture different macroscopic behaviors, such as free vs. constrained walking (with a treadmill or a metronome), or pathological behaviors. Indeed, the level of LRA in series of stride durations of healthy people was decreased when walking on a

Postprint

treadmill (18, 19) or to the rhythm of a metronome (20). Other clinical studies have shown that specific patient populations – such as people affected by Parkinson's or Huntington's diseases (21) – have a decreased level of LRA in series of stride durations as compared to a control group.

The exact physiological origin of LRA is still largely debated. Several studies hypothesized that its presence in a given system reflects its intrinsic complexity, arising from the coordination of its multiple components and subsystems. In particular, locomotion indeed results from the complex interaction between neural, muscular, and mechanical subsystems that interact with each other towards the emergence of rich dynamic tasks (23, 24). Moreover, this system is redundant, i.e., its components have similar functions and can therefore be used alternately for the same task (24). This makes the locomotor system adaptable and robust to disturbances, whether external or internal. Indeed, humans need to continuously adapt every step in response to incoming proprioceptive feedbacks, corresponding for example to minor variations in the walking surface or to the inherent noise in the neuromuscular system (18). A complementary perspective to this theory is given by the Goal Equivalent Manifold framework proposed by Dingwell and colleagues (25). It builds upon the postulate that there exist an infinite number of manners to perform a step, by varying some features such as speed, step length, or duration. In this context, humans are able to adapt their walking features from stride to stride, while adopting minimum intervention strategies to regulate them, in order to achieve a specific walking goal while enhancing task performance. Such a goal could be for example maintaining a constant walking speed in the case of treadmill walking (25, 26), or a constant gait cycle timing in the case of walking with a metronome (25), or a constant step width during overground walking (27). The model of (25) managed to reproduce LRA in these various conditions with a low state dimension, thus challenging the requirement of complexity postulated by (23, 24).

The aim of the present paper is thus to study the impact of delivering an oscillator-based walking assistance with a wearable active pelvis orthosis on the level of LRA in series of stride durations of a healthy aging population, i.e., people over 55 years. Delivering walking assistance can indeed be considered equivalent as adding a constraint to walking, like a treadmill or a metronome, since it intrinsically tends to assist the gait pattern. However, in the perspective of being used in rehabilitation with pathological populations such as people with Parkinson's disease, who already have a level of LRA below the one of a healthy population, it is relevant to provide robotic assistance that will not amplify this trend, or that could even mitigate it. Indeed, recent modeling studies predicted that our assistance framework could have a positive effect on the level of LRA, at least for people with pathological levels (28, 29). In that respect, we hypothesize that the adaptive assistance provided by the orthosis used in this study will not lower the LRA level as a metronome or treadmill would do. Indeed, the assistance algorithm has been specifically designed to keep the wearer in control of their main gait features. The experiments in this study were conducted in a semi-ecological environment, i.e., overground instead of on a treadmill, in order to isolate the effects of gait constrained by our walking assistance.

MATERIALS AND METHODS

The experimental protocol of this study has the ClinicalTrials.gov identifier NCT04314973 (registered on 11 April 2020).

Postprint

Participants

A total of ten healthy participants aged between 55 and 77 years (mean 63.10, SD 6.12 years, 6 females) participated in this study. This age range was chosen with a perspective of using this group as a control one for experiments with patients with Parkinson's disease, that has been identified as developing between the ages of 55 and 65 (30). Exclusion criteria were the inability to walk independently or less than 20 consecutive minutes, and the presence of any neurological disease or other medical condition that could directly affect gait. This study was conducted at the Mounier Sports Center (Brussels, Belgium), and under the approval of the local ethical committee (Comité d'Ethique Hospitalo-Facultaire des Cliniques universitaires Saint-Luc, EudraCT n. 2019-002048-26), in compliance with the declaration of Helsinki. Participants provided written consent prior to data collection and were left free to leave the study at any moment.

Procedures



Fig. 1. The Active Pelvis Orthosis (IUVO S.r.l., Pisa, Italy).

Subjects wore a bilateral wearable Active Pelvis Orthosis (APO, Fig. 1), which assists flexion and extension movements of both hips. This orthosis is the commercial version of the prototype developed in the framework of the CYBERLEGs and CYBERLEGsPlusPlus research projects (31), now brought to a commercial product by the company IUVO (Pisa, Italy, www.iuvo.company). This device weighs about 6 kg, and it can inject a peak assistive torque of 16 Nm with a bandwidth of 17.5 Hz.

Subjects were asked to walk while wearing the orthosis in transparent mode and under three different assistive conditions. For each condition, subjects were asked to walk freely at their comfortable speed in a sports hall during 15 min. They had to follow a rectangular path of 7 m × 12 m with rounded corners, so that the gait is as steady as possible throughout the acquisition, for LRA assessment purposes. The walking session was performed in a quiet environment so as to keep the attentional cost of walking as low as possible (32). After a period where subjects can adapt their gait to the device's assistance, the acquisition started and speed steadiness was verified by timing the time taken by the subject to complete each lap, and delivering qualitative instructions to adapt walking speed if needed.

Post Print

Hip kinematics and kinetics

The orthosis itself acquired some signals with onboard sensors at 100 Hz. The hip flexion-extension angle was recorded by an absolute encoder embedded in the orthosis on both sides. The injected torque was indirectly quantified by measuring the deformation of a torsional spring also integrated in the device actuation chain (31). In the present paper, only data from the right leg will be analyzed, since inter-stride intervals time series were obtained only from that side.

The torque injected was first normalized by the weight of each subject. Then, hip angle and torque signals were divided into individual gait cycles using the maximum hip extension angle as separation event between cycles. The hip angle was also time-differentiated and then used to compute the power exerted by the orthosis over each cycle, i.e., $P = T\,\mathrm{d}x/\mathrm{d}t$, with P the power [W/kg], T the injected torque [Nm/kg], and x the hip angular position [rad]. Finally, the energy injected to the hip by the orthosis was obtained by integrating this power over each gait cycle. The hip range of motion (ROM) and the energy injected to the hip were computed for each gait cycle, then averaged over all cycles. In addition, the occurrence time of the maximum hip flexion angle and of the maximum torque injected at the hip during the gait cycle were computed as the time difference between the beginning of a cycle and the following maximum in the angle or torque signal respectively, normalized by the duration of the corresponding cycle.

Stride intervals computation

The sagittal shank angular velocity was recorded at a sample rate of 500 Hz using an inertial measurement unit (NGIMU, x-io Technologies, Bristol, UK) fixed just above the right external malleolus using a Velcro strap, with its x-axis oriented in the direction of walking.

A zero crossings detection algorithm was used in order to obtain inter-stride time series, i.e., the time between two consecutive heel strikes of the same foot. The negative-going zero crossing occurring just after the maxima in the sagittal shank angular velocity indicates the end of a swing phase (33), corresponding to heel strike events (Fig. 2).

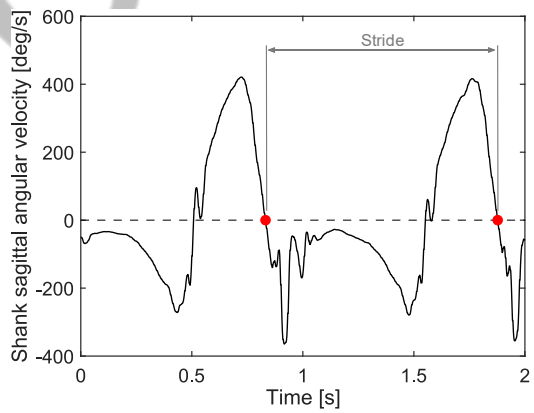


Fig. 2. Detection of zero crossings with negative slope corresponding to the end of the swing phase. The duration of a given stride is taken as the time interval between two consecutive crossings.

The maxima of the signal were first identified. Then, the first sign change occurring after each of these maxima was detected. Finally, a linear interpolation was performed between both adjacent points to obtain

Postprint

the most accurate zero crossing detection. When all these events were detected, the inter-stride time series was obtained by differentiating the series of these time-stamped events. For the following analyses, the first and last 30 strides of each recording were discarded, in order to analyze steady-state behavior only. The series of stride durations contained at least 512 points, which is a typical requirement for LRA assessment (34).

Spatiotemporal gait data

From the inter-stride time series, the mean stride duration was computed. Walking speed per lap was computed by dividing the lap distance (38 m) by the time taken by subjects to walk through each of them. Finally, the mean stride length over the whole trial was obtained by taking the product between the mean stride duration and the mean walking speed. These last two metrics were then normalized by dividing by the leg length of each subject.

Long-range autocorrelations assessment

A more advanced metric can be obtained from the inter-stride time series: the level of LRA, which can be quantified by the fractal scaling exponent α. To compute this exponent, we used the Adaptive Fractal Analysis (AFA). This is a method similar to the more common Detrended Fluctuation Analysis (DFA) method. However, AFA has the advantages of not being limited to stationary time series and of being more robust than DFA when using short time series (35).

This method is described in details elsewhere (35, 36). Briefly, the integrated time series was divided into overlapping subseries of length w. Second order quadratic polynomials were then fitted to each subseries and pasted together to obtain a globally smooth trend signal. The residual variance $F(w)$ of the difference between this global trend and the original series was reported for several subseries sizes w, ranging from 5 to the first power of 2 smaller than $N/2$ by steps of 2, where N is the length of the time series. To obtain evenly spaced values of w in a logarithmic scale, the range of $\log_2(w)$ was divided into a series of intervals of equal length with a step size of 0.5, and the points falling within each interval were averaged. This range of window sizes was determined as the most appropriate to handle non-stationary time series, i.e., with low frequency trends. Finally, the fractal exponent α was obtained as the slope of the linear regression of $\log_2\big(F(w)\big)$ as a function of $\log_2(w)$.

Several cases can be found (35):

- $0 < \alpha < 0.5$: the time series is stationary and contains long-range anticorrelations, which means that increases in the signal are more likely to be followed by decreases;
- $\alpha = 0.5$: the time series is a random process or a white noise;
- $0.5 < \alpha < 1$: the time series is stationary and contains long-range correlations, which means that increases in the signal are more likely to be followed by increases;
- $\alpha = 1$: the time series is a pink or 1/f noise, i.e., a process with a power spectral density inversely proportional to the frequency of the signal;
- $\alpha > 1$: the time series is non-stationary.

Postprint

Experimental conditions

The walking assistance used for these experiments is based on the use of adaptive oscillators, such that the device continuously synchronizes with the recorded hip trajectories, and adapts to changes in these signals. The torque provided by the APO in this study is obtained following the methods explained in (31):

$$T = k\big(\hat{x}(\varphi + \Delta\varphi) - \hat{x}(\varphi)\big) \quad (1)$$

where k is a tunable virtual stiffness [Nm/rad], φ is the gait phase estimated by the oscillators and $\Delta\varphi$ is a tunable phase lead, both expressed in percentage of gait cycle, and $\hat{x}(\varphi)$ is the hip position [rad] estimated by the *n* oscillators according to the following equation (37):

$$\hat{x}(\varphi) = \sum_{i=1}^{n} a_i \sin(\varphi_i) + a_0 \quad (2)$$

where the phase φ_i, the frequency ω, the amplitude a_i and the offset a_0 are learned by the internal dynamics of the n adaptive oscillators, see equations (3) to (6) in the Appendix for more details.

This assistance can be adjusted using three parameters. The first one is the virtual stiffness k, which determines the magnitude of the assistance. It was adjusted as a function of the weight of the subject, i.e., so that the peak torque at the hips was equal to 0.1 Nm/kg for each condition described hereunder, corresponding to a comfortable and safe level of assistance as reported in (38). The second one is the phase lead $\Delta\varphi$, determining how far in advance the signal of the hip is predicted for computing the injected torque. Finally, the third parameter is the learning time constant τ [s] of the adaptive oscillators, characterizing the time it takes to the oscillators to adapt to changes in gait features, see equation (7) in the Appendix.

A total of four conditions were tested:

(o) Transparent mode, where the exoskeleton applied no torque;
(i) Baseline condition: $\tau = 4$ s and $\Delta\varphi = 1\%$;
(ii) Increased oscillators memory: $\tau = 10$ s and $\Delta\varphi = 1\%$;
(iii) Increased phase lead: $\tau = 4$ s and $\Delta\varphi = 10\%$.

The transparent mode was selected as the control setting to ensure that the weight does not affect the analysis of the presence of LRA in series of stride durations, thereby making the conditions comparable. A value of $\tau = 4$ s corresponds to the basic setting of the device, while a value of $\tau = 10$ s was chosen in order to challenge the results of a previous modeling study (28), predicting that increasing the oscillators memory increases the level of LRA in time series. A value of $\Delta\varphi = 1\%$ is the smallest possible value to have assistance provided, while a value of $\Delta\varphi = 10\%$ shifts the assistance torque profile backward in time, and thus increases the correlation between the actual hip angular speed and assistive torque.

Conditions were randomized for each participant, and they were blinded to the three assistance conditions. Two conditions were tested each day over two days, to avoid fatigue effects. The minimum break between the two conditions of the same day was five minutes, and could be increased upon request from the participant. All subjects completed all the conditions.

Postprint

Statistical analysis

Data were processed with Matlab version R2019a (RRID:SCR_001622), and statistical tests were performed in R version 3.6.2 (RRID:SCR_001905).

Conditions (o) and (i) were compared with each other and with the conditions (ii) and (iii), in terms of each metric presented above. Linear mixed models were fitted to the different studied metrics, with subjects as random effects and the four conditions as fixed effects (39). An analysis of variance (ANOVA) was then performed on these models, using a Kenward-Roger's approximation to degrees of freedom (40). If the *p*-value of this test was lower than 0.05, Tukey's tests for multiple pairwise comparisons were performed, using the Benjamini-Hochberg correction (41).

The variances of the α exponent in the four conditions were also compared with a Levene's test (42), in order to determine whether there is a normalizing effect on subjects' behavior with the assistance of the device. If significant, this test was followed by pairwise Levene's tests, and a Benjamini-Hochberg correction was applied on the resulting *p*-values.

For graphical representation of all these metrics, inter-subject variability is represented through the standard error of the mean, computed as the standard deviation divided by the number of subjects. Only the inter-subject variability of the α exponent is represented by the standard deviation, since this parameter is compared across the different conditions.

RESULTS

On average, subjects took 675.30 strides (SD 68.19) in condition (o), 674 strides (SD 99.51) in condition (i), 688 strides (SD 62.94) in condition (ii), and 718.80 strides (SD 66.22) in condition (iii).

Kinematics profiles are shown in Fig. 3 for a representative subject (left column) and averaged across all subjects (right column). As expected, it can be observed that the torque in transparent mode, and therefore also the power injected at the hip, are close to zero. For the assistive modes, the maximum torque applied to the hips was approximately equal to 6 Nm for the representative subject, as their weight is about 60 kg. It can also be observed that the amplitude of the hip joint angle is larger in the three assistive modes than in the transparent mode. Finally, it can be noted that the maximum flexion angle in condition (iii) is slightly shifted in time compared to both other assistive conditions, and this also shifts the peak torque applied to the hip.

As expected, the statistical tests showed that the mean energy injected during a cycle was higher for the three assistive conditions, i.e., 7.74 J/kg (SD 2.06), 7.96 J/kg (SD 2.52) and 7.25 J/kg (SD 1.64) respectively, than in the transparent mode, i.e., 0.14 J/kg (SD 0.06) ($p \leq 0.001$). The time occurrence of the maximum hip flexion angle (Fig. 4a) was smaller in condition (ii) compared to the transparent mode, i.e., 30.04 (SD 2.36) versus 31.58 (SD 1.46) % of gait cycle ($p \leq 0.01$), and larger in condition (iii) than in (i), i.e., 32.55 (SD 1.47) versus 30.51 (SD 2.06) % of gait cycle ($p \leq 0.001$). The time occurrence of the maximum torque injected at the hip (Fig. 4b) was smaller in condition (iii) than in (i), i.e., 15.27 (SD 1.47) versus 19.02 (SD 2.06) % of gait cycle ($p \leq 0.001$). Concerning the hip ROM (Fig. 4c), the statistical tests revealed that its mean value over cycles was significantly higher in conditions (i) and (ii) than in the transparent mode, i.e., 54.45° (SD 6.52) and

Postprint

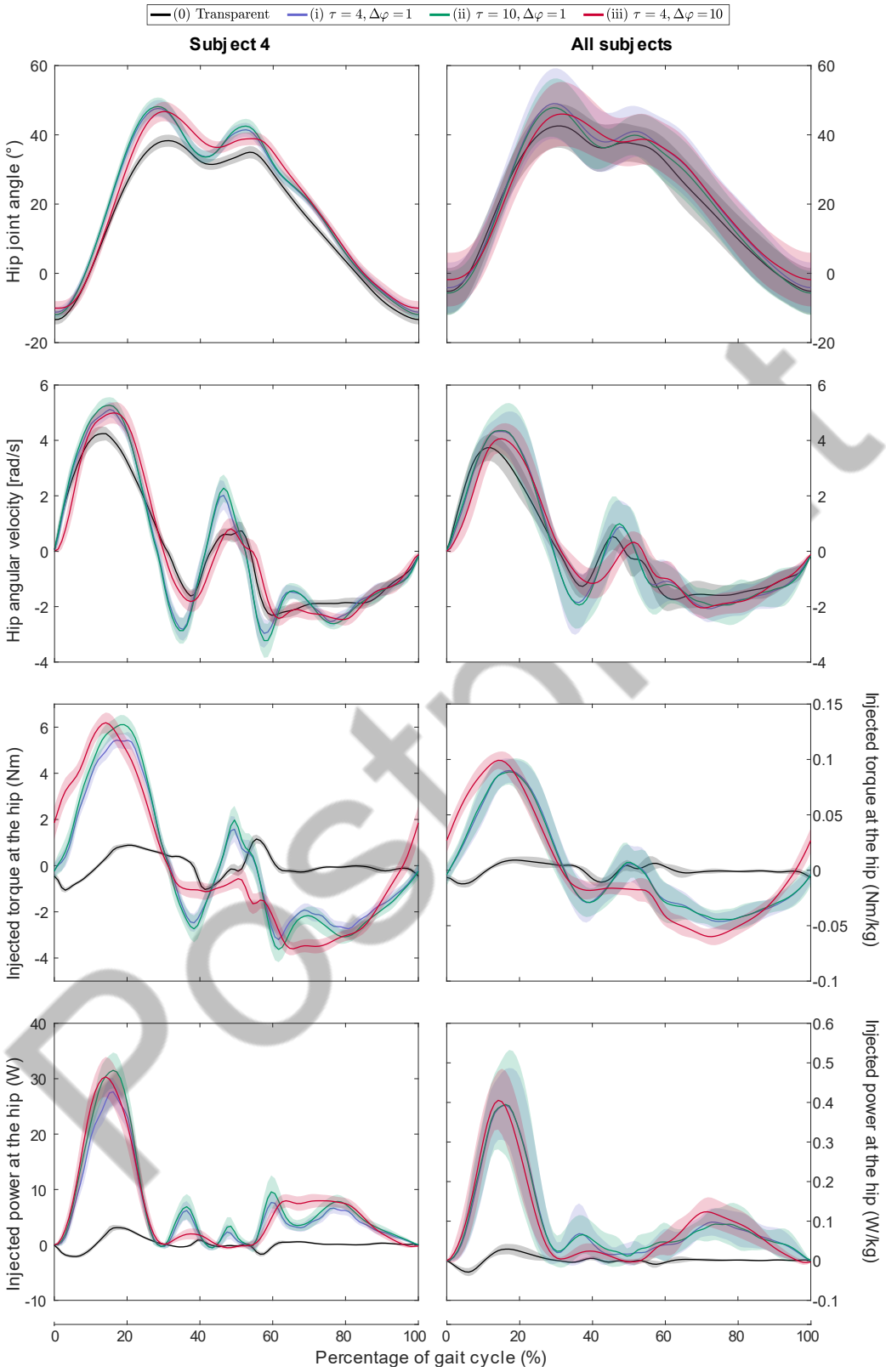


Fig. 3. Top to bottom: angular position and velocity of the right hip, delivered torque and power for subject 4 (left) and all subjects (right) in transparent mode and in the three different assistive conditions. Signals were time-normalized over the gait cycle. Solid lines represent the mean and shaded areas represent the standard deviation over all gait cycles (left) or across subjects (right).

Postprint

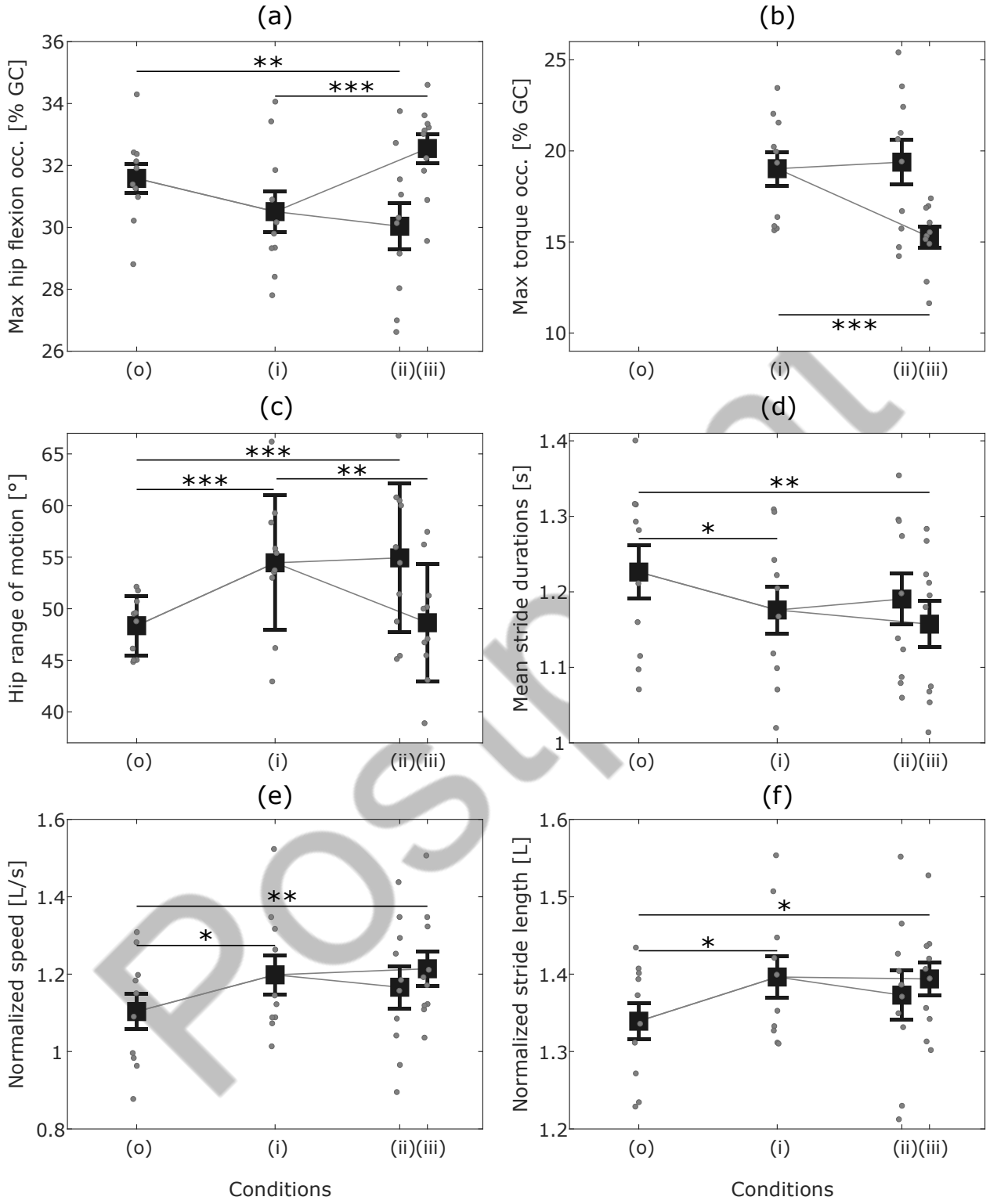


Fig. 4. (a) Maximum hip flexion time occurrence and (b) maximum torque injected time occurrence in percentage of the gait cycle (GC), (c) right hip range of motion, (d) mean stride duration, (e) normalized gait speed, and (f) normalized stride length, as a function of the experimental conditions, i.e., (o) transparent mode, (i) $\tau = 4$ s and $\Delta\varphi = 1\%$, (ii) $\tau = 10$ s and $\Delta\varphi = 1\%$, and (iii) $\tau = 4$ s and $\Delta\varphi = 10\%$. Squares represent the mean across participants and whiskers indicate standard error of the mean. Each point corresponds to individual data of one participant in each condition. Significance levels of the multiple comparison tests: *** $p \leq 0.001$, ** $p \leq 0.01$, * $p \leq 0.05$.

Postprint

54.92° (SD 7.22) respectively versus 48.35° (SD 2.86) ($p \leq 0.001$). On the other hand, it was significantly lower in condition (iii) than in (i), i.e., 48.64° (SD 5.65) versus 54.45° (SD 6.52) ($p \leq 0.01$). Regarding the spatiotemporal gait metrics (Fig. 4d-f), the statistical tests indicated an increase in gait speed and stride length between the conditions (i) and (iii) and the transparent mode, i.e., 1.20 L/s (SD 0.16) and 1.21 L/s (SD 0.14) respectively versus 1.10 L/s (SD 0.14) ($p \leq 0.05$) for speed, and 1.40 L (SD 0.16) and 1.39 L (SD 0.14) respectively versus 1.34 L (SD 0.14) ($p \leq 0.05$) for stride length. Moreover, a decrease in stride duration was observed between the same conditions and the transparent mode, i.e., 1.18 s (SD 0.10) and 1.16 s (SD 0.10) respectively versus 1.23 s (SD 0.11) ($p \leq 0.01$).

Finally, concerning the level of LRA in the inter-stride time series (Fig. 5), indicated by the α exponent, no significant differences were found between conditions, either with respect to means or standard deviations, with values of 0.78 (SD 0.14) in condition (o), 0.75 (SD 0.10) in condition (i), 0.78 (SD 0.08) in condition (ii), and 0.70 (SD 0.10) in condition (iii). The *p*-value was 0.11 for the ANOVA test, and 0.78 for the Levene's test. We carried out a similar analysis with another LRA assessment method, i.e., the adapted version of the Power Spectral Density analysis $^{low}PSD_{we}$ (43), and this did not yield significant results either.

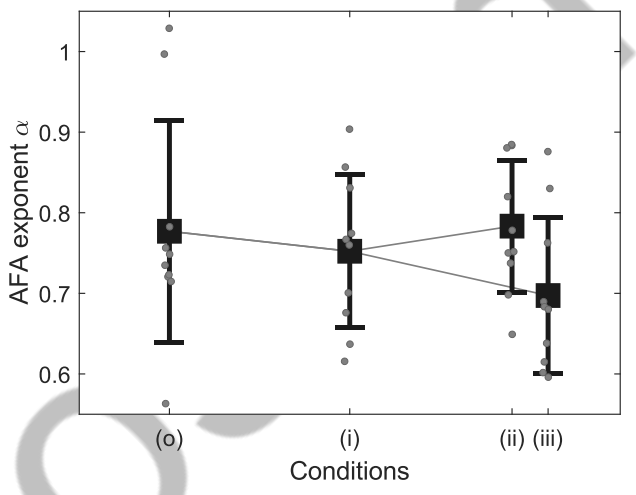


Fig. 5. AFA exponent α, reflecting the level of LRA, as a function of the experimental conditions, i.e., (o) transparent mode, (i) $\tau = 4$ s and $\Delta\varphi = 1\%$, (ii) $\tau = 10$ s and $\Delta\varphi = 1\%$, and (iii) $\tau = 4$ s and $\Delta\varphi = 10\%$. Squares represent the mean across participants and whiskers indicate standard deviation across participants. Each point corresponds to individual data of one participant in each condition. No pairwise comparison was significant.

DISCUSSION

This section discusses the main results reported previously, and interpret them as a function of the different experimental conditions.

Our results confirm that the orthosis provided energy in the three assistive conditions compared to the transparent mode. No distinction is made between conditions, because the virtual stiffness k was tuned for each individual condition in order to reach a similar peak torque, and because the velocity profile did not significantly change across conditions.

Post-print

This injected energy induced a change in the behavior of the user. Indeed, the hip ROM, walking speed and stride length were significantly increased between condition (i) and the transparent mode, accompanied by a decrease in stride duration. The change in hip kinematics could be explained by the assistance compensating for the loss of hip muscles force due to aging. Indeed, previous results established that the lower-limb maximum muscle force and power decrease by 8% per decade between the ages of 25 and 75 (44). More precisely, a decrease of 22% in the maximum isometric torque of hip flexor muscle for people aged around 75, compared to healthy young adults, has previously been reported (45). The energy injected by the device might thus have helped users to retrieve a larger hip ROM during walking. It might also have helped users to increase their cadence – observed via the decreased stride duration – and their stride length. Both of these changes are known strategies for increasing walking speed (46).

Moreover, two other assistive conditions have been tested, focusing on the potential influence of key parameters in the oscillator-based framework, namely its memory τ and its phase lead $\Delta\varphi$. Different changes can be observed in the previously mentioned gait metrics depending on which assistive parameter was increased. In condition (ii), increasing the oscillators memory mitigated the effect of the assistance on the spatiotemporal metrics, i.e., stride duration, gait speed, and stride length. This is possibly due to the fact that with a larger memory, the device is less compliant with kinematic changes across steps, leaving the user with less authority over these gait metrics. Nevertheless, this interpretation should be taken with caution, since there is no significant difference between this condition and the transparent (o) or baseline conditions (i); while the latter two are significantly different. On the other hand, condition (iii) showed that increasing the phase lead mitigated the effects on the hip ROM. Indeed, it can be observed in Fig. 3 that although the maximum flexion angle for all subjects is higher than in the transparent mode, the extension angle is smaller, thus giving rise to no significant increase in ROM. This can be explained by the different assistive pattern observed in this condition compared to condition (i), since the maximum hip flexion angle occurred later in the gait cycle, and the maximum torque was injected earlier.

The study by d'Elia and colleagues (38) is a good benchmark to ours, since they used the same APO and the same oscillator-based assistance framework than in our study, with the same assistive parameters as in our condition (iii). Their experiments involved five healthy young adults, who walked on a treadmill at three different speeds and under five different conditions, i.e., without the APO, in transparent mode, and in three assistive modes with increasing assistance level k (peak torque at the hips ≤ 0.14 Nm/kg). They showed that the assistance had no effect on step length and cadence, and that the hip ROM increased when wearing the device in transparent and assistive modes compared to without the APO. These results are thus not entirely consistent with ours, especially concerning the spatiotemporal metrics. A key difference between both protocols is that the one of d'Elia and colleagues was performed on a treadmill, thus imposing the walking speed and de facto inducing kinematic constraints. In our case, participants performed overground walking. They were thus free to adapt all features of their gait to the provided assistance, and even to walk at different forward speeds between conditions.

Postprint

In contrast, previous studies reporting the effects of an overground training program with wearable hip orthoses have shown similar results to ours with respect to spatiotemporal metrics. A first example is the study of Sanz-Morère and colleagues (13), which analyzed the effect of another assistive mode of the same APO, consisting in injecting a torque profile computed from Gaussian curves, and tested on transfemoral amputees. These authors reported an increase in gait speed and in gait symmetry after a four-week training program with the device. Another device using the same principle of assistance, namely the Gait Enhancing and Motivating System (GEMS, Samsung Electronics, Suwon, South Korea), also led to increased gait speed, cadence and stride length in people with hemiparetic stroke, after 10 training sessions, half of them performed on a treadmill (47). Finally, a study with the Stride Management Assist (SMA®, Honda R&D, Tokyo, Japan) (10), adapting the provided torque according to a target walk ratio (step length/cadence), showed that a six to eight week training program led to increased gait speed, cadence, step time and stride length with post-stroke people.

A limitation of our experiment highlighted by these previous studies is the lack of investigation of the effect of assistance on the metabolic cost of walking, although this is a key parameter capturing walking rehabilitation in the elderly. Nevertheless, the study of Sanz-Morère and colleagues (13) using the same APO showed that, with a level of peak torque similar to the one provided in our three assistive conditions, the energy cost of transport was decreased, measured through a portable gas analyzer. This remains to be verified in our protocol.

As opposed to the spatiotemporal gait metrics, no assistive condition had a significant effect on the level of LRA in series of stride durations. Our participants had good baseline mobility and therefore a level of LRA corresponding to healthy people of the same age (22, 48). Some studies have hypothesized that a decrease in LRA in inter-stride time series would indicate a more random temporal organization of this series, and thus would be a marker of gait instability, in particular in elderly (49) or patients with Parkinson's disease (32). LRA-related metrics have therefore been proposed as a valuable clinical tool for assessing mobility and gauging the effectiveness of therapeutic interventions (18), associated with other metrics such as the coefficient of variation of stride durations, and questionnaires assessing fear of falling and postural stability (32). The present study showed that with an assistance based on adaptive oscillators, the capacity to display levels of LRA observed during unconstrained walking is preserved in healthy aging people. Regardless of whether the presence of LRA reflects a complex organization of physiological subsystems (23, 24), or the trace of a goal-equivalent manifold control (25), our results show that this natural dynamics is not affected by the assistance we tested. It also determined the influence of the different parameters of the assistance on the spatiotemporal gait metrics. These observations are important in the perspective of using this orthosis and this assistive framework for the rehabilitation of pathological populations such as patients with Parkinson's disease. Indeed, several studies have shown that the LRA level of these patients is deteriorated (22). Moreover, it has been shown that the gait of these patients is characterized by a slower walking speed, a lower cadence, as well as shorter strides, which makes them more prone to fall (50). These metrics are precisely among those improved by the assistance method tested in the present paper, as shown on healthy aging people. In addition, a three-month overground training program with the SMA orthosis on patients with Parkinson's disease (11)

Postprint

showed an increased exercise endurance and walking speed, as well as improvements in motor symptoms of this disease. Obtaining similar results with our approach would therefore offer great perspectives for people suffering from locomotion disorders induced by a neurodegenerative disease.

There are a number of limitations that need to be addressed regarding the current study. Firstly, it was conducted as an open-label uncontrolled trial, which can induce observer and reporting biases. Secondly, the sample size of our study was relatively small, reducing the power of the study. Finally, as the hip angle was given by the orthosis, the results about the hip ROM should be taken with caution since there can be a relative movement between the subject's hip and the orthotic one.

In conclusion, an oscillators-based wearable walking assistance can improve several gait metrics in healthy aging people, such as hip ROM, stride duration, gait speed, and stride length, by adequately selecting the assistive parameters. Moreover, this assistance does not deteriorate the level of LRA present in series of stride durations of these people. This result is of interest for the field of locomotion, since it is uncommon to observe that external constraints do not alter the level of LRA in series of stride durations. Besides, combining these two features is appealing for the development of a rehabilitation device for people having a decreased level of LRA, as it is the case with some neurodegenerative diseases.

Postprint

APPENDIX: Adaptive oscillators

The dynamic state equations of the *n* adaptive oscillators, used in equation (2), are given by (37, 51):

$$\dot{\varphi}_i(t) = \omega(t)i + \nu_\varphi \frac{F(t)}{\sum a_i(t)} \cos\big(\varphi_i(t)\big) \tag{3}$$

$$\dot{\omega}(t) = \nu_\omega \frac{F(t)}{\sum a_i(t)} \cos\big(\varphi_1(t)\big) \tag{4}$$

$$\dot{a}_i(t) = \eta F(t) \sin\big(\varphi_i(t)\big) \tag{5}$$

$$\dot{a}_0 = \eta F(t) \tag{6}$$

with the estimated phases $\varphi_i(t)$, the frequency $\omega(t)$, amplitudes $a_i(t)$ and offset $a_0(t)$.

All these variables converge to the corresponding ones of the measured input $x(t)$ by using as teaching signal the error between the real and estimated inputs: $F(t) = x(t) - \hat{x}(t)$.

In those equations, the learning gains are computed by (52):

$$\eta = \frac{2}{\tau}; \nu_\omega = \frac{20}{\tau^2}; \nu_\varphi = \sqrt{24.2\nu_\omega} \tag{7}$$

where η is the amplitude gain, ν_ω is the frequency gain, ν_φ is the phase gain, and τ is a time constant determining the time for the oscillator to learn the input signal features.

Abbreviations

AFA: Adaptive Fractal Analysis; ANOVA: Analysis of Variance; APO: Adaptive Pelvis Orthosis; DFA: Detrended Fluctuation Analysis; LRA: Long-Range Autocorrelations; ROM: Range of Motion.

DATA AVAILABILITY

The data that support the findings of this study are available from Össur but restrictions apply to the availability of these data, which were used under license for the current study, and so are not publicly available. Data are however available from the authors upon reasonable request and with permission of Össur.

ACKNOWLEDGMENTS

We thank Alexandre Jacquemain (UCLouvain) for his help in the statistical analysis, and all the volunteers who agreed to participate in the experiments.

GRANTS

This work was supported by the Fonds de la Recherche Scientifique - FNRS under Grant n° PDR T.0200.19: PaDAWAn project.

Postprint

DISCLOSURES

The authors declare that they have no competing interests.

AUTHOR CONTRIBUTIONS

VO managed the recruitment of participants, conducted the experiments and performed data analysis. VO and RR equally contributed to the design of the study, the writing and editing of the manuscript, and approved the final manuscript.

REFERENCES

1. **Marchal-Crespo L**, **Riener R**. Chapter 16 - Robot-assisted gait training. In: *Rehabilitation Robotics*. 2018, p. 227–240.

2. **van Dellen F**, **Labruyère R**. Settings matter: a scoping review on parameters in robot-assisted gait therapy identifies the importance of reporting standards. *J Neuroeng Rehabil* 19: 40, 2022. doi: 10.1186/s12984-022-01017-3.

3. **Alwardat M**, **Etoom M**, **Al Dajah S**, **Schirinzi T**, **Di Lazzaro G**, **Sinibaldi Salimei P**, **Mercuri NB**, **Pisani A**. Effectiveness of robot-assisted gait training on motor impairments in people with Parkinson's disease: a systematic review and meta-analysis. *Int J Rehabil Res* 41: 287–296, 2018. doi: 10.1097/MRR.0000000000000312.

4. **Lorusso M**, **Tramontano M**, **Casciello M**, **Pece A**, **Smania N**, **Morone G**, **Tamburella F**. Efficacy of overground robotic gait training on balance in stroke survivors: A systematic review and meta-analysis. *Brain Sci* 12: 713, 2022. doi: 10.3390/brainsci12060713.

5. **Kerdraon J**, **Previnaire JG**, **Tucker M**, **Coignard P**, **Allegre W**, **Knappen E**, **Ames A**. Evaluation of safety and performance of the self balancing walking system Atalante in patients with complete motor spinal cord injury. *Spinal Cord Ser Cases* 7: 71, 2021. doi: 10.1038/s41394-021-00432-3.

6. **Morris L**, **Cramp M**, **Turton A**. User perspectives on the future of mobility assistive devices: Understanding user's assistive device experiences and needs. *J Rehabil Assist Technol Eng* 9: 20556683221114790, 2022. doi: 10.1177/20556683221114790.

7. **Rodríguez-Fernández A**, **Lobo-Prat J**, **Font-Llagunes JM**. Systematic review on wearable lower-limb exoskeletons for gait training in neuromuscular impairments. *J Neuroeng Rehabil* 18: 22, 2021. doi: 10.1186/s12984-021-00815-5.

8. **Qiu S**, **Pei Z**, **Wang C**, **Tang Z**. Systematic review on wearable lower extremity robotic exoskeletons for assisted locomotion. *J Bionic Eng* 20: 436–469, 2022. doi: 10.1186/s12984-021-00815-5.

9. **Dzeladini F**, **van den Kieboom J**, **Ijspeert A**. The contribution of a central pattern generator in a reflex-based neuromuscular model. *Front Hum Neurosci* 8: 371, 2014. doi: 10.3389/fnhum.2014.00371.

10. **Buesing C**, **Fisch G**, **O'Donnell M**, **Shahidi I**, **Thomas L**, **Mummidisetty CK**, **Williams KJ**, **Takahashi H**, **Rymer WZ**, **Jayaraman A**. Effects of a wearable exoskeleton stride management assist system (SMA®) on spatiotemporal gait characteristics in individuals after stroke: a randomized controlled trial. *J Neuroeng Rehabil* 12: 69, 2015. doi: 10.1186/s12984-015-0062-0.

Postprint

11. **Kawashima N**, **Hasegawa K**, **Iijima M**, **Nagami K**, **Makimura T**, **Kumon A**, **Ohtsuki S**. Efficacy of wearable device gait training on Parkinson's disease: A randomized controlled open-label pilot study. *Intern Med J* 61: 2573–2580, 2022. doi: 10.2169/internalmedicine.8949-21.

12. **Pan Y-T**, **Kang I**, **Joh J**, **Kim P**, **Herrin KR**, **Kesar TM**, **Sawicki GS**, **Young AJ**. Effects of bilateral assistance for hemiparetic gait post-stroke using a powered hip exoskeleton. *Ann Biomed Eng* 51: 410–421, 2022. doi: 10.1007/s10439-022-03041-9.

13. **Sanz-Morère CB**, **Martini E**, **Meoni B**, **Arnetoli G**, **Giffone A**, **Doronzio S**, **Fanciullacci C**, **Parri A**, **Conti R**, **Giovacchini F**, **Friðriksson Þ**, **Romo D**, **Crea S**, **Molino Lova R**, **Vitiello N**. Robot-mediated overground gait training for transfemoral amputees with a powered bilateral hip orthosis: a pilot study. *J Neuroeng Rehabil* 18: 111, 2021. doi: 10.1186/s12984-021-00902-7.

14. **Mooney LM**, **Rouse EJ**, **Herr HM**. Autonomous exoskeleton reduces metabolic cost of human walking during load carriage. *J Neuroeng Rehabil* 11: 80, 2014. doi: 10.1186/1743-0003-11-80.

15. **Shin SY**, **Hohl K**, **Giffhorn M**, **Awad LN**, **Walsh CJ**, **Jayaraman A**. Soft robotic exosuit augmented high intensity gait training on stroke survivors: a pilot study. *J Neuroeng Rehabil* 19: 51, 2022. doi: 10.1186/s12984-022-01034-2.

16. **Haufe FL**, **Schmidt K**, **Duarte JE**, **Wolf P**, **Riener R**, **Xiloyannis M**. Activity-based training with the Myosuit: a safety and feasibility study across diverse gait disorders. *J Neuroeng Rehabil* 17: 135, 2020. doi: 10.1186/s12984-020-00765-4.

17. **Warlop TB**, **Bollens B**, **Crevecoeur F**, **Detrembleur C**, **Lejeune TM**. Dynamics of revolution time variability in cycling pattern: voluntary intent can alter the long-range autocorrelations. *Ann Biomed Eng* 41: 1604–1612, 2013. doi: 10.1007/s10439-013-0834-2.

18. **Terrier P**, **Dériaz O**. Kinematic variability, fractal dynamics and local dynamic stability of treadmill walking. *J Neuroeng Rehabil* 8: 12, 2011. doi: 10.1186/1743-0003-8-12.

19. **Hollman JH**, **Watkins MK**, **Imhoff AC**, **Braun CE**, **Akervik KA**, **Ness DK**. Complexity, fractal dynamics and determinism in treadmill ambulation: Implications for clinical biomechanists. *Clin Biomech* 37: 91–97, 2016. doi: 10.1016/j.clinbiomech.2016.06.007.

20. **Hausdorff JM**, **Purdon P**, **Peng CK**, **Ladin Z**, **Wei JY**, **Goldberger AL**. Fractal dynamics of human gait: stability of long-range correlations in stride interval fluctuations. *J Appl Physiol* 80: 1448–1457, 1996. doi: 10.1152/jappl.1996.80.5.1448.

21. **Hausdorff JM**, **Lertratanakul A**, **Cudkowicz ME**, **Peterson AL**, **Kaliton D**, **Goldberger AL**. Dynamic markers of altered gait rhythm in amyotrophic lateral sclerosis. *J Appl Physiol* 88: 2045–2053, 2000. doi: 10.1152/JAPPL.2000.88.6.2045.

22. **Hausdorff JM**, **Cudkowicz ME**, **Firtion R**, **Wei JY**, **Goldberger AL**. Gait variability and basal ganglia disorders: stride-to-stride variations of gait cycle timing in Parkinson's Disease and Huntington's Disease. *Mov Disord* 13: 428–437, 1998. doi: 10.1002/mds.870130310.

23. **Delignières D**, **Marmelat V**. Fractal fluctuations and complexity: current debates and future challenges. *Crit Rev Biomed Eng* 40: 485–500, 2012. doi: 10.1615/critrevbiomedeng.2013006727.

24. **Delignières D**, **Marmelat V**. Degeneracy and long-range correlations. *Chaos* 23: 043109, 2013. doi: 10.1063/1.4825250.

Post Print

25. **Dingwell JB**, **John J**, **Cusumano JP**. Do humans optimally exploit redundancy to control step variability in walking? *PLoS Comput Biol* 6: e1000856, 2010. doi: 10.1371/journal.pcbi.1000856.

26. **Dingwell JB**, **Bohnsack-McLagan NK**, **Cusumano JP**. Humans control stride-to-stride stepping movements differently for walking and running, independent of speed. *J Biomech* 76: 144–151, 2018. doi: 10.1016/j.jbiomech.2018.05.034.

27. **Render AC**, **Kazanski ME**, **Cusumano JP**, **Dingwell JB**. Walking humans trade off different task goals to regulate lateral stepping. *J Biomech* 119: 110314, 2021. doi: 10.1016/j.jbiomech.2021.110314.

28. **Otlet V**, **Ronsse R**. Predicting the effects of oscillator-based assistance on stride-to-stride variability of Parkinsonian walkers. In: *2022 International Conference on Robotics and Automation (ICRA)*. Philadelphia, PA, USA: 2022, p. 8083–8089.

29. **Vandamme C**, **Otlet V**, **Ronsse R**, **Crevecoeur F**. Model of gait control in Parkinson's disease and prediction of robotic assistance. *IEEE Trans Neural Syst Rehabil Eng* 31: 1374–1383, 2023. doi: 10.1109/TNSRE.2023.3245286.

30. **Rizek P**, **Kumar N**, **Jog MS**. An update on the diagnosis and treatments of Parkinson disease. *Can Med Assoc J* 188: 1157–1165, 2016. doi: 10.1503/cmaj.151179.

31. **Giovacchini F**, **Vannetti F**, **Fantozzi M**, **Cempini M**, **Cortese M**, **Parri A**, **Yan T**, **Lefeber D**, **Vitiello N**. A light-weight active orthosis for hip movement assistance. *Rob Auton Syst* 73: 123–134, 2015. doi: 10.1016/j.robot.2014.08.015.

32. **Warlop TB**, **Detrembleur C**, **Bollens B**, **Stoquart G**, **Crevecoeur F**, **Jeanjean A**, **Lejeune TM**. Temporal organization of stride duration variability as a marker of gait instability in Parkinson's disease. *J Rehabil Med* 48: 865–871, 2016. doi: 10.2340/16501977-2158.

33. **Hundza SR**, **Hook WR**, **Harris CR**, **Mahajan S V**, **Leslie PA**, **Spani CA**, **Spalteholz LG**, **Birch BJ**, **Commandeur DT**, **Livingston NJ**. Accurate and reliable gait cycle detection in Parkinson's disease. *IEEE Trans Neural Syst Rehabil Eng* 22: 127–137, 2014. doi: 10.1109/TNSRE.2013.2282080.

34. **Warlop T**, **Bollens B**, **Detrembleur C**, **Stoquart G**, **Lejeune T**, **Crevecoeur F**. Impact of series length on statistical precision and sensitivity of autocorrelation assessment in human locomotion. *Hum Mov Sci* 55: 31–42, 2017. doi: 10.1016/j.humov.2017.07.003.

35. **Hollman JH**, **Lee WD**, **Ringquist DC**, **Taisey C**, **Ness DK**. Comparing adaptive fractal and detrended fluctuation analyses of stride time variability: Tests of equivalence. *Gait Posture* 94: 9–14, 2022. doi: 10.1016/j.gaitpost.2022.02.019.

36. **Riley MA**, **Bonnette S**, **Kuznetsov N**, **Wallot S**, **Gao J**. A tutorial introduction to adaptive fractal analysis. *Front Physiol* 3: 371, 2012. doi: 10.3389/fphys.2012.00371.

37. **Yan T**, **Parri A**, **Ruiz Garate V**, **Cempini M**, **Ronsse R**, **Vitiello N**. An oscillator-based smooth real-time estimate of gait phase for wearable robotics. *Auton Robots* 41: 759–774, 2016. doi: 10.1007/s10514-016-9566-0.

38. **D'Elia N**, **Vanetti F**, **Cempini M**, **Pasquini G**, **Parri A**, **Rabuffetti M**, **Ferrarin M**, **Molino Lova R**, **Vitiello N**. Physical human-robot interaction of an active pelvis orthosis: towards ergonomic assessment of wearable robots. *J Neuroeng Rehabil* 14: 29, 2017. doi: 10.1186/s12984-017-0237-

Postprint

y.

39. **Brown VA**. An introduction to linear mixed-effects modeling in R. *Adv Methods Pract Psychol Sci* 4: 1–19, 2021. doi: 10.1177/2515245920960351.

40. **Kenward MG**, **Roger JH**. Small sample inference for fixed effects from restricted maximum likelihood. *Biometrics* 53: 983–997, 1997. doi: 10.2307/2533558.

41. **Benjamini Y**, **Hochberg Y**. Controlling the false discovery rate: A practical and powerful approach to multiple testing. *J R Stat Soc Ser B* 57: 289–300, 1995. doi: 10.1111/j.2517-6161.1995.tb02031.x.

42. **Levene H**. Robust tests for equality of variances. In: *Contributions to Probability and Statistics: Essays in Honor of Harold Hotelling*. 1960, p. 278–292.

43. **Eke A**, **Herman P**, **Bassingthwaighte JB**, **Raymond GM**, **Percival DB**, **Cannon M**, **Balla L**, **Ikrényi C**. Physiological time series: distinguishing fractal noises from motions. *Eur J Physiol* 439: 403–415, 2000. doi: 10.1007/s004249900135.

44. **Grimmer M**, **Riener R**, **Walsh CJ**, **Seyfarth A**. Mobility related physical and functional losses due to aging and disease – a motivation for lower limb exoskeletons. *J Neuroeng Rehabil* 16: 2, 2019. doi: 10.1186/s12984-018-0458-8.

45. **Dean JC**, **Kuo AD**, **Alexander NB**. Age-related changes in maximal hip strength and movement speed. *J Gerontol* 59A: 286–292, 2004. doi: 10.1093/gerona/59.3.m286.

46. **Ruiz Garate V**, **Parri A**, **Yan T**, **Munih M**, **Molino Lova R**, **Vitiello N**, **Ronsse R**. Walking assistance using artificial primitives: A novel bioinspired framework using motor primitives for locomotion assistance through a wearable cooperative exoskeleton. *IEEE Robot Autom Mag* 23: 83–95, 2016. doi: 10.1109/MRA.2015.2510778.

47. **Lee H-J**, **Lee S-H**, **Seo K**, **Lee M**, **Chang WH**, **Choi B-O**, **Ryu G-H**, **Kim Y-H**. Training for walking efficiency with a wearable hip-assist robot in patients with stroke: A pilot randomized controlled trial. *Stroke* 50: 3545–3552, 2019. doi: 10.1161/STROKEAHA.119.025950.

48. **Bollens B**, **Crevecoeur F**, **Detrembleur C**, **Guillery E**, **Lejeune T**. Effects of age and walking speed on long-range autocorrelations and fluctuation magnitude of stride duration. *Neuroscience* 210: 234–242, 2012. doi: 10.1016/j.neuroscience.2012.02.039.

49. **Herman T**, **Giladi N**, **Gurevich T**, **Hausdorff JM**. Gait instability and fractal dynamics of older adults with a "cautious" gait: why do certain older adults walk fearfully? *Gait Posture* 21: 178–185, 2005. doi: 10.1016/j.gaitpost.2004.01.014.

50. **Creaby MW**, **Cole MH**. Gait characteristics and falls in Parkinson's disease: a systematic review and meta-analysis. *Park Relat Disord* 57: 1–8, 2018. doi: 10.1016/j.parkreldis.2018.07.008.

51. **Ronsse R**, **Vitiello N**, **Lenzi T**, **van den Kieboom J**, **Carrozza MC**, **Ijspeert AJ**. Human-robot synchrony: Flexible assistance using adaptive oscillators. *IEEE Trans Biomed Eng* 58: 1001–1012, 2011. doi: 10.1109/TBME.2010.2089629.

52. **Ronsse R**, **De Rossi SMM**, **Vitiello N**, **Lenzi T**, **Carrozza MC**, **Ijspeert AJ**. Real-time estimate of velocity and acceleration of quasi-periodic signals using adaptive oscillators. *IEEE Trans Robot* 29:

Postprint

783–791, 2013. doi: 10.1109/TRO.2013.2240173.

Postprint